ELSEVIER

Journal of Nuclear Materials 241–243 (1997) 564–568

journal of nuclear materials

Investigation of interaction between MeV-ions and first wall from neutron and γ-ray measurements in JT-60U

T. Kondoh *, Y. Kusama, H. Kimura, M. Saigusa, T. Fujii, S. Moriyama, M. Nemoto, K. Tobita, A. Morioka, K. Nagashima, T. Nishitani

Japan Atomic Energy Research Institute, Naka Fusion Research Establishment, 801-1 Mukouyama, Naka-machi, Naka-gun, Ibaraki-ken 311-01, Japan

Abstract

Loss of MeV-energy protons to the first wall during H-minority second harmonic ion cyclotron range of frequency (ICRF) heating has been measured for the first time by neutron signals emitted by $^{11}B(p,n)^{11}C$ reaction in B_4C coated divertor tiles and boronized tiles in the JT-60U tokamak. Since the reaction has a threshold energy of 3.0 MeV, the neutron signal indicates loss of fast protons whose energy is more than 3 MeV. Measurements of gamma-ray lines emitted from reaction between the fast protons and plasma impurities are also used for measurements of confined protons accelerated up to 5 MeV.

Keywords: JT-60U; Tokamak; Fast particle losses; RF heating

1. Introduction

The loss mechanism of energetic particles to the first wall is one of the issues to be investigated for a tokamak fusion reactor. Escaping fast ions were measured by MeV-ion detectors in TFTR [1,2] and in JET [3,4]. Heat deposition on the first wall due to fast particles was also investigated in plasmas heated by neutral beams [5] and by ion cyclotron range of frequency (ICRF) [6] using an infrared TV camera in JT-60U.

In this paper, we propose new diagnostics of MeV-proton loss, which detects neutrons produced through $^{11}B(p,n)^{11}C$ reaction between lost protons and boron at the first wall. Since the reaction has a threshold energy of 3.0 MeV, the neutron signal indicates loss of fast protons with the energy more than 3 MeV. In the experiments, fast protons were produced by ICRF heating [7,8] and a temperature of the fast protons was estimated by intensity ratios of gamma-ray lines.

2. Experimental set-up

In the JT-60U tokamak, most of plasma facing surfaces are composed of carbon tiles; carbon-fiber composite (CFC) is used for divertor plates and all the other tiles are made of isotropic graphite. Two toroidal rows of the divertor plates were B_4C coated CFC tiles: with thicknesses of 100 μm and 300 μm [9]. The first wall has been boronized several times using decaborane ($B_{10}H_{14}$) [10]. The average thickness of the boron layer is estimated to be 300 nm from consumed decaborane. The frequency of the ICRF was set at 116 MHz corresponding to the second harmonic resonance frequency of protons at 3.8 T.

The schematic view of the neutron and γ-ray measurement system is shown in Fig. 1. Neutron measurements were performed with absolutely calibrated ^{235}U fission chambers [11]. Three neutron detectors were placed on the torus midplane, just outside the toroidal field coils, each at different toroidal positions.

Time-resolved γ-ray spectra in an energy range from 0.5 through 20 MeV were measured by a NaI(Tl) scintillator of 12.7 cm in diameter and 12.7 cm in length surrounded by a 50 cm thick polyethylene and 30 cm thick

* Corresponding author. Tel.: +81-292 70 7347; fax: +81-292 70 7339; e-mail: kondoh@naka.jaeri.go.jp.

PII S0022-3115(96)00565-X

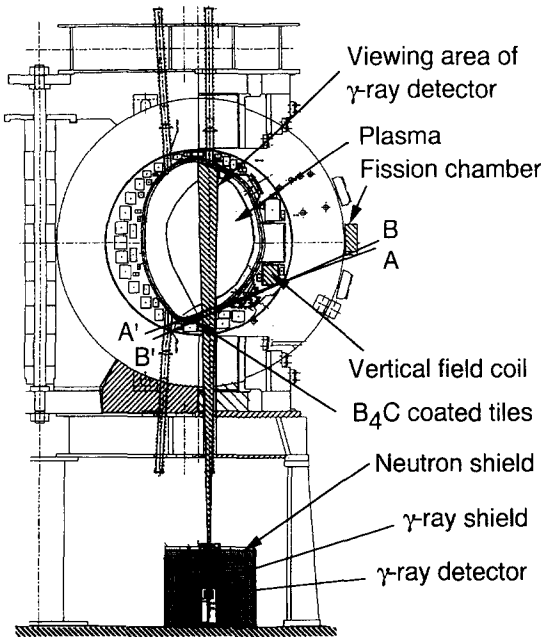

Fig. 1. Layout of the neutron and γ-ray detectors on JT-60U. The three neutron detectors are placed on the torus midplane at different toroidal positions. The viewing area of the γ-ray detector is collimated at the center region of the plasma.

lead shield. The signal is processed by CAMAC and pulse height analyzed into 256 channels every 50 ms. Whereas the fission chambers measures global neutron emission, the viewing area of the γ-ray detector is collimated to see the center area of the plasma.

Experiments were carried out with H-minority second harmonic ICRF heating with He as working gas. Experimental conditions were plasma current of $I_P = 2$–3.5 MA, toroidal field of $B_T = 3.8$ T at the center of the plasma, line averaged electron density of $\bar{n}_e = (1.3\text{–}3.6) \times 10^{19}$ m^{-3}, and injected ICRF power of $P_{IC} \leq 6$ MW.

3. Neutron and γ-ray radiation

During the H-minority ICRF experiments in JT-60U, neutrons were emitted from $^{11}B(p,n)^{11}C$ reaction between confined fast protons and impurity boron in plasmas [8]. This reaction has a threshold energy of 3.0 MeV and the cross-section of up to 0.1 b. Boron originating from the coatings of the first wall is one of the impurity species of JT-60U.

In the ICRF heated plasmas, γ-rays are produced when protons are accelerated to a few MeV or greater. Measured γ-ray spectra in the ICRF heating experiment are shown in Fig. 2. Gamma-ray lines of 2.1 MeV and 4.4 MeV were observed and they were originated from $^{11}B(p,p')^{11}B$ and $^{12}C(p,p')^{12}C$ reactions (inelastic collision of protons with

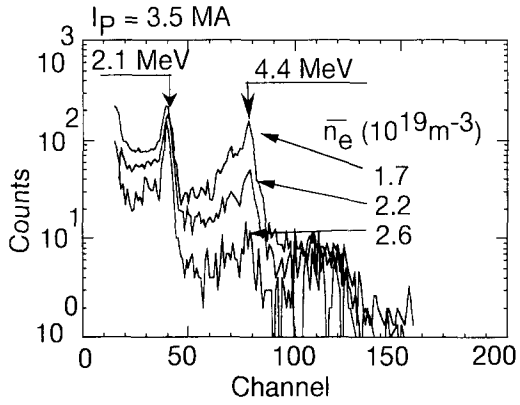

Fig. 2. γ-ray spectra in the 2nd harmonic ICRF heating experiment for three values of electron density. $I_P = 3.5$ MA.

impurity ions), respectively. The energy of the γ-ray is determined from the first excited state of the nucleus. The cross-section of the reactions measured by Huus [12] and Dyer [13], reaches up to 1 b and the reactions have threshold proton energies of 2.5 and 5.0 MeV, respectively. It was confirmed from the threshold energy that the protons were accelerated more than 5 MeV.

Fig. 3 shows intensities of the γ-ray lines and neutron emission rate divided by ICRF power against $T_e^{1.5}/\bar{n}_e$, which is proportional to the slowing-down time of fast protons, where the value of T_e is central electron temperature. Intensities of the lines and neutrons depend strongly on $T_e^{1.5}/\bar{n}_e$ as shown in the figure. The tail temperature of protons, T_p, is roughly estimated from an intensity ratio between the γ-ray lines of 2.1 and 4.4 MeV with an

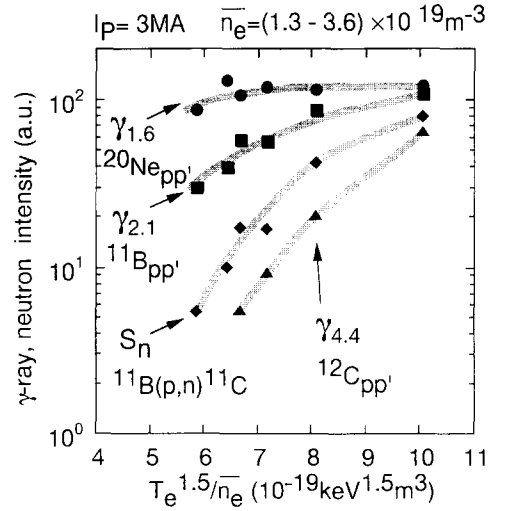

Fig. 3. Intensities of the γ-ray lines and neutron versus $T_e^{1.5}/\bar{n}_e$ which is proportional to the slowing down time of the fast protons. The tail temperature of protons increases with increasing $T_e^{1.5}/\bar{n}_e$.

assumption of the energy distribution of $f \sim \exp(-E_p/T_p)$. The tail temperature increased from 0.6 to 1 MeV as the electron density decreased from 3.6 to 1.3×10^{19} m^{-3}.

4. Neutron and γ-ray behavior during giant sawtooth activities

In JT-60U, giant sawteeth are observed during the application of high power ICRF. This section describes experimental results on the giant sawtooth activities observed from the neutron and γ-ray measurements.

Experimental conditions were $I_P = 3.5$ MA, $\bar{n}_e = 2.2 \times 10^{19}$ m^{-3} and $P_{IC} = 5.3$ MW. Typical time traces of plasma parameters are shown in Fig. 4: ICRF power (P_{IC}), soft X-ray, diamagnetic stored energy (W_{dia}), intensities of C VI (33.7 Å) and B V (48.6 Å), 2.1 MeV and 4.4 MeV γ-ray counts and neutron yield of channel 2 and 3. Neutron signals originate from the $^{11}B(p,n)^{11}C$ reaction. In this experimental condition, the neutrons originating from d–d reaction can be neglected.

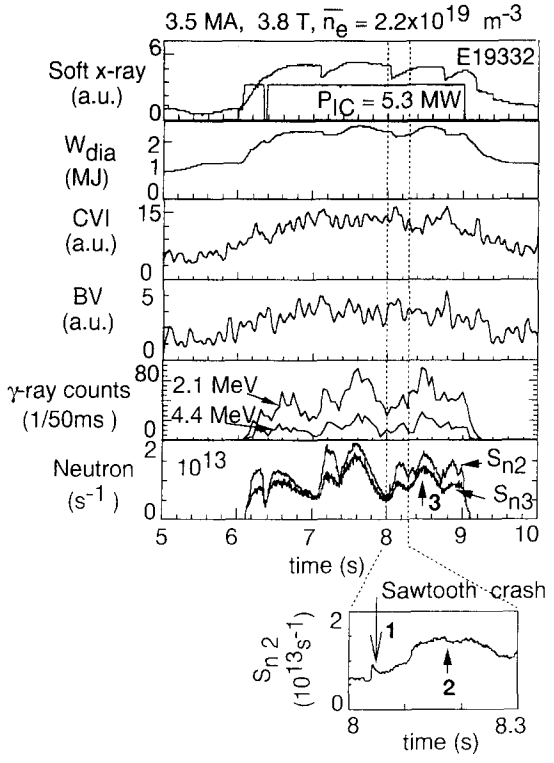

Fig. 4. Time evolution of γ-ray and neutron signal during giant sawtooth activities in ICRF heated discharge. Soft X-ray signal, 2.1 and 4.4 MeV γ-ray counts, intensities of C VI (33.7 Å) and B V (48.6 Å) and neutron signals of S_{n2} (wall + plasma) and S_{n3} (plasma) are presented. $I_P = 3.5$ MA, $\bar{n}_e = 2.2 \times 10^{19}$ m^{-3}. After a monster crash, three kinds of peaks in the neutron signal were observed.

After each giant sawtooth crash, three kinds of peaks in the neutron yield were observed: (i) the first rapid peak at $t = 8.03$ s just after the sawtooth crash indicated by an arrow in the bottom figure; rise time, Δt_{rise} was the response time of the detector (2 ms), (ii) the second peak at $t = 8.2$ s ($\Delta t_{rise} \approx 0.1$ s), (iii) the third peak at $t = 8.5$ s ($\Delta t_{rise} \approx 0.5$ s). The γ-ray signals of 2.1 and 4.4 MeV also showed the second and third peaks. The γ-ray detector, however, could not observe the first rapid peaks because its time resolution was only 50 ms.

The first peaks in neutron signal can be considered to be emitted by reaction between lost protons and the first wall, as discussed in the following section. The second peaks are considered to be due to enhanced influx of boron impurities accompanied with the giant sawtooth crash because the γ-ray signals also increase. This is in accordance with VUV and visible spectroscopic measurements of the main and divertor plasmas in which a large increment of impurity lines accompanied with a giant crash was observed [14]. The third peaks are due to increases in fast protons; stored energy as well as γ-ray lines also increases in this phase [8].

As shown in the γ-ray signals in the second peaks, γ-ray spectroscopy may become a powerful tool to measure impurities in the plasma core where VUV or visible spectroscopy cannot measure.

5. Estimation of neutron intensity emitted from the first wall

The proton loss was measured with neutron detectors during ICRF heating. Experimental conditions were $I_P = 3$ MA, $\bar{n}_e = 2.1 \times 10^{19}$ m^{-3} and $P_{IC} = 3.1$ MW. Temporal evolutions of γ-ray and neutron signals are shown in Fig. 5: from the top, count of γ-ray lines of 1.6 MeV ($^{20}Ne(p,p')^{20}Ne$) and 2.1 MeV, neutron signals of the three detectors, S_{n1}–S_{n3}, S_{n2}–S_{n3} and soft X-ray intensity. In this shot, neon gas was puffed to confirm that the γ-ray originated from the plasma. The impurity influx accompanied with a sawtooth crash was not observed in this experiment.

After a sawtooth crash, the neutron signal increases. However, both of the 1.6 MeV and 2.1 MeV γ-ray signals drop. Since the intensity of 1.6 MeV γ-ray showed weak dependence on electron temperature, the drop after the crash suggests a decrease in the population of fast protons or impurity ions in the central region of the plasma.

The γ-ray detector views the central region of the plasma. Meanwhile, the fission chambers measure global neutron emission from the plasma as well as from the wall. The response of the detectors to the neutron yield from the plasma was considered to be equal because of toroidal symmetry of plasma parameters and careful calibration of the detectors [11]. However, the three neutron signals at

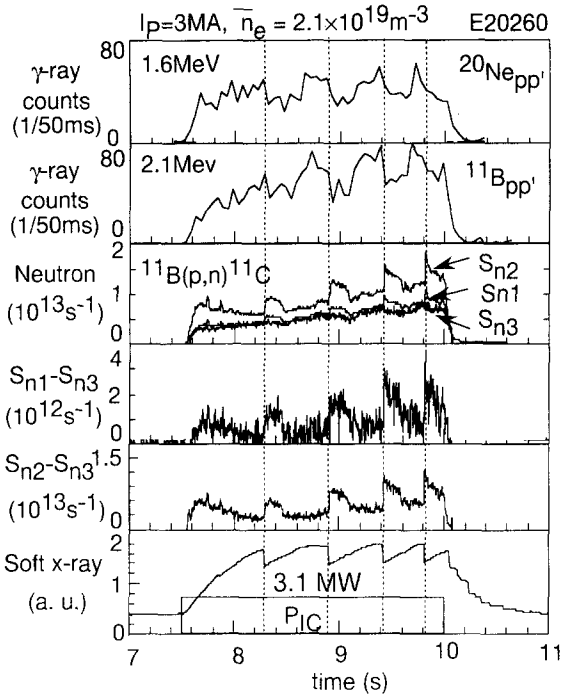

Fig. 5. Gamma-ray and neutron behavior during sawtooth activities in ICRF heated discharge with Ne gas puff. 1.6 and 2.1 MeV γ-ray counts, neutron signals of three fission chambers and soft X-ray signal are presented. $I_P = 3$ MA, $\bar{n}_e = 2.1 \times 10^{19}$ m^{-3}. After a crash, neutron signals from the wall ($S_{n1} - S_{n3}$ and $S_{n2} - S_{n3}$) increased.

different toroidal positions exhibited different behavior as shown in Fig. 5. Therefore, the difference in the three signals showed local neutron emission from the first wall in which fast protons reacted with boron.

The neutron signal of channel i can be described as follows:

$$S_{ni} = S_n^{\text{plasma}} + \eta_i Y_n^{\text{wall}} \quad (1)$$

where S_n^{plasma} and Y_n^{wall} are neutron yields from the plasma and from the wall. Factor η_i is efficiency of the detector i to the neutrons from the wall: for a uniform emission $\eta_i = 1$, for a localized emission in front of the detector $\eta_i = 6$, and for at 80 degrees toroidal position from the detector $\eta_i = 0.3$, which is estimated from point efficiencies of the detectors measured using ^{252}Cf neutron source [11]. Since there was no rise in S_{n3} after the sawtooth crash as shown in Fig. 5, S_{n3} is considered to be dominated by S_n^{plasma}. Then we define neutron emission from the first wall $S_n^{\text{wall}} \equiv S_{n2} - S_{n3}$ ($= \eta_2 Y_n^{\text{wall}}$). As shown in Fig. 5, comparing with drops of 1.6 MeV and 2.1 MeV γ-rays just after a sawtooth crash, rapid increases in S_n^{wall} indicates an increase in loss of the fast protons to the wall.

It is difficult to identify the location of neutron emission with only three neutron detectors. However, the increase in neutron signal after the sawtooth crash and the difference among three channels were not observed before the installation of B_4C coated divertor tiles in February 1993. Therefore, origin of the emission is considered to be the B_4C coated tiles. One possible reason for the different behavior among three detectors is that the positions of the detectors are not exactly the same: the neutron detector 3 (S_{n3}) is placed 10 cm above the detector 2 (S_{n2}). For the detector 3, the B_4C coated tiles are hidden behind a vertical field coil as indicated by a line B–B′ in Fig. 1. However, the detector 2 can see the B_4C coated tiles as indicated by a line A–A′.

6. Discussions

In the previous section, it was shown that some fraction of the neutron signals originated from the reaction between the lost protons and boron at the first wall. In this section, we examine capability of the neutron diagnostics as a MeV-ion loss detector.

Fig. 6(a), (b) show $S_n^{\text{plasma}}/P_{IC}$ and S_n^{wall}/P_{IC} against $T_e^{1.5}/\bar{n}_e$ for three values of plasma current, respectively. These data were obtained during periods without MHD activity. Though neutron signals from the wall increase with decreasing I_P, neutron signals from the plasma do not change with I_P. This result indicates that MeV-proton loss to the divertor tile is not the dominant loss process in the ICRF plasma. The loss process of the MeV-ion to the divertor tiles coated with B_4C is considered to be an ICRF induced ripple trapped loss [6] or an ICRF induced loss

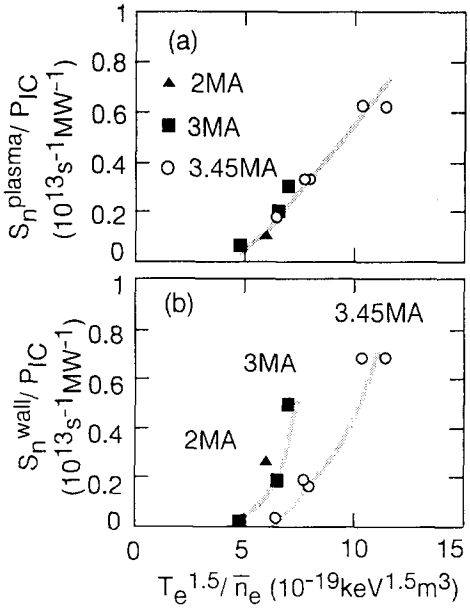

Fig. 6. (a) Neutron signal from the plasma divided by ICRF power ($S_n^{\text{plasma}}/P_{IC}$) and (b) neutron signal from the first wall divided by ICRF power (S_n^{wall}/P_{IC}).

from a counter-passing orbit [2], both of which is consistent with the I_p dependence of the neutron intensities.

Next, loss power to the wall is estimated from neutron signals. Neutron signals from the wall can be written in the form,

$$S_n^{wall} = n_{boron}^{wall} \delta_{boron} \int \Gamma_p \sigma \, d\nu \int^{wall} \eta \, ds \qquad (2)$$

where Γ_p, σ, n_{boron}^{wall} and δ_{boron} are the proton loss flux, cross-section of the $^{11}B(p,n)^{11}C$ reaction, boron density in the target wall and boron thickness of the target, respectively. If we represent the cross-section of the reaction for protons with energy more than 3 MeV to be $\bar{\sigma}$, then $S_n^{wall} \approx n_{boron}^{wall} \delta_{boron} \Gamma_p^* \bar{\sigma} A_{wall} \eta$, where Γ_p^* is a flux of protons whose energy is more than 3 MeV. Lost power of the protons to the wall can be represented as

$$P_{loss}^* = \int \Gamma_p(\nu) E_p d\nu \int^{wall} ds \approx A_{wall} \Gamma_p^* E_p^*$$

where E_p and E_p^* are the energy of a lost proton and the averaged energy of the lost protons, respectively. The insertion of Eq. (2) yields $P_{loss}^* = S_n^{wall} E_p / (\bar{\sigma} n_{boron}^{wall} \delta_{boron} \eta)$.

Assuming the origin of the neutron is 100 μm thick, B_4C coated tiles and protons have a monochromatic energy of $E_p = 4$ MeV, we obtain $P_{loss} = 190$ kW (for $\eta = 0.3$) and 9.6 kW (for $\eta = 6$) for $S_n^{wall} = 10^{13}$ s^{-1}. If the exact values of η and δ_{boron} are known, we can measure lost power accurately. Furthermore, if two-dimensional images of the neutron emission are obtained, spatial profile of the lost protons with energy of more than 3 MeV will be identified.

7. Summary

We have developed new fast proton loss diagnostics using the neutron signals of $^{11}B(p,n)^{11}C$ reaction between boron in the first wall and fast protons during ICRF heating in JT-60U. Assuming the detection efficiency of the neutron and proton energy, we estimate lost power of the fast protons to the wall to be 9.6–190 kW for $S_n^{wall} = 10^{13}$ s^{-1}. If the exact values of the detection efficiency of the neutrons and position of the hitting point at the first wall are known, this method may become a powerful tool to measure lost protons to the wall.

Acknowledgements

We would like to express our appreciation to the members of JT-60 team, especially members of the RF Facility Division, Large Tokamak Experiment Division I and II, for experimental support and helpful discussions. We also acknowledge Mr. H. Harano of University of Tokyo for efficiency calculation of the γ-ray detectors and Dr. R. Yoshino, Dr. M. Mori and Dr. H. Kishimoto for their continuous support.

References

[1] S.J. Zweben et al., Nucl. Fusion 30 (1990) 1551.
[2] D.S. Darrow et al., Nucl. Fusion 36 (1996) 1.
[3] E.V. Carruthers et al., J. Nucl. Mater. 176–177 (1990) 1027.
[4] G.J. Sadler et al., Fusion Technol. 18 (1990) 556.
[5] K. Tobita et al., Phys. Rev. Lett. 69 (1992) 3060.
[6] Y. Kusama et al., J. Nucl. Mater. 220 (1995) 438.
[7] M. Saigusa et al., Plasma Phys. Control. Fusion 37 (1995) 295.
[8] H. Kimura et al., Phys. Lett. A 199 (1995) 86.
[9] S. Higashijima et al., J. Nucl. Mater. 220–222 (1995) 375.
[10] M. Saidoh et al., Fusion Eng. Des. 22 (1993) 271.
[11] T. Nishitani et al., Rev. Sci. Instrum. 63 (1992) 5270.
[12] T. Huus et al., Phys. Rev. 91 (1953) 599.
[13] P. Dyer et al., Phys. Rev. C 23 (1981) 1865.
[14] M. Ueda et al., in: Proc. Int. Conf. on Plasma Phys (1994) p. 109.